INNSPUB

International Journal of Biosciences | IJB |
ISSN: 2220-6655 (Print), 2222-5234 (Online)
http://www.innspub.net
Vol. 14, No. 1, p. 271-283, 2019

RESEARCH PAPER OPEN ACCESS

# A multifunctional poly (vinylidene fluoride) nanocomposites reinforced with single walled carbon nanotubes and iron oxide nanoparticles

**Muhammad Arif[1*], Mohsan Nawaz[1], Saira Bibi[1], Saddiqa Bigum[1], Shakeel Zeb[2], Qaribullah[1], Hameed Ur Rehman[3], Wajid Ullah[3], Ikram Ullah[3], Muhammad Ikramullah[4], Zia Ul Islam[5], Zohra Aftab Bokharee[5]**

[1]*Department of Chemistry, Hazara University, Mansehra, KP, Pakistan*

[2]*Department of Analytical chemistry, Institute of Chemistry, State University of Sau Paulo (UNESP)*

[3]*Department of Chemistry, Kohat University of Science & Technology, KUST, Kohat-26000, KP, Pakistan*

[4]*Department of Chemistry, Shaheed Benazir Butto University Sheringal Upper Dir KP, Pakistan*

[5]*Department of Botany, Kohat University of Science & Technology, KUST, Kohat-26000, KP, Pakistan*

**Key words:** Multifunctional Poly (Vinylidene fluoride), Nanocomposites Reinforced, Carbon Nanotubes, Iron Oxide Nanoparticles.

http://dx.doi.org/10.12692/ijb/14.1.271-283 Article published on January 26, 20199

## Abstract

This research work elaborates the synthesis and characterization of PVDF nanocomposite films reinforced with $Fe_3O_4$ NPs and γ-SWCNTs. Nanocomposite film were synthesized through solution casting method, DMF (Dimethyleformamide) used as a solvent. For proper dispersion of nanofiller, samples were sonicated followed by reflux. Different types of PVDF nanocomposite were synthesized by adding different weight percent of nanofiller (0%, 0.03% γ-SWCNTs, 0.01% $Fe_3O_4$, 0.03% γ-SWCNTs/0.01% $Fe_3O_4$) to PVDF matrix. Results obtained from the analysis of Scanning electron microscopy (SEM), Fourier transform infrared spectrometry (FT-IR), X-rays diffraction (XRD) were very informative for the phase change of PVDF from α-phase to β-phase, Thermogravimetric analysis (TGA) shows the thermal stability of the system, while impedance spectroscopy shows the enhancement in electrical and dielectrical properties of PVDF by incorporating nanofillers.

* **Corresponding Author:** Muhammad Arif ✉ muharif878@gmail.com

**Introduction**

Polyvinylidene fluoride (PVDF) with semi-crystalline character is pure thermoplastic and a non-reactive polymer having five crystalline phases known as: α, β, γ, δ, ε-phases[A. J. Lovinger, 1983], containing fluorine atom bonded to carbon atom. This material is categorized by an extraordinary resistivity to bases, acid as well as solvent. It is produced by the combination of the vinylidene difluoride ($H_2C=CF_2$)[P. Martins, 2014]. PVDF is piezoelectric substance and having greater stability than any other polymer and behave same like of other fluoropolymers in similar environment. No chemical degradation or oxidation occurs by continuous exposure to high temperature up to 149°C [X. Gu,2006, H. Kawai,1969]. The property of piezoelectricity make it desired substance for many applications like headphones, microphones and sensors[Y. Fu,2005]. The most important phase i.e β-phase, having two chains in all-trans (TTTT) planar zigzag structure are connected into an orthorhombic unit cell. In all five phases, β-phase has highest spontaneous polarization. Many research effort have used to obtained β-phase due to their strong ferroelectrics[J. Bergman Jr, 1971] pyroelectricty and piezoelectricity[T. Furukawa,1989,V. Sencadas,2006]. The morphology of the polymer is affected by the addition of nanofillers and also having the effect on the mechanical properties of the polymer. In this regard CNTs and ferrite is used as additive and have marked effect on the morphology, piezoelectricity, and thermal as well as on the mechanical properties of PVDF, which can be used in electronics, actuators and sensors [O. Bajpai,2015,S. Begum,2016]. The effect of CNTs on the morphology of PVDF have being studied by Zhang *et al.* [S. Zhang, 2005] used coagulation method for the preparation of PVDF/CNTs composite, Wang *et al.* [M. Wang, 2007] used melt mixing method for the preparation of nanocomposite, Manna and Nadi [S. Manna, 2010] using solution casting and metl-mixing method for composite preparation, Levi *et al.* [N. Levi,2004] achieve composite of PVDF with addition of CNTs by solution casting method Kim *et al.* [G. H. Kim, 2009]formed composite by solution casting method. These all studies were performed for change in crystallinity as well as for the enhancement of β-phase PVDF. Magnetite nanomaterial have become the most advanced research material in the field of chemistry because magnetite nanoparticles play an important role in increasing the properties of composite material. Among Nano sized material iron oxide are very important due to magnetic properties, biodegradability, biocompatibility and low cost as well as having interesting role in the enhancement of nanocomposite properties due to its application in electronics, optical and mechanical devices[W. Eerenstein,2006,J. Kumar,2006, G. A. Prinz, 1998]. PVDF/$Fe_3O_4$composite shows superparamagnetic nature with the presence of $Fe_3O_4$ Nanoparticles, while the maximum saturation magnetization were found to be 30.8 emu/g [X. Wang, 2012]. Incomposite film of PVDF/$Fe_3O_4$which are prepared by solution casting method, it was found that by the inclusion of Nanoparticles ($Fe_3O_4$) significant increase in crystallinity of PVDF and β-phase content[T. Prabhakaran,2013 20]. While decrease in crystallinity and increase in conductivity were also be reported by some authors [A. S. Bhatt, 2011].

In order to investigate the effect of CNTs addition on the crystallization, the mechanical, electrical and thermal properties of PVDF/CNTs composites much work has been done. In addition to this the incorporation of third phase in the form of inorganic nanoparticles has been explored with the objective to increase the multifunctionality of the prepared ternary nanocomposites. Like the advanced work on ternary nanocomposites it has been shown that the addition of graphene oxide enhance the thermal conductivity [W.-b. Zhang, 2015], The Dielectric permittivity were greatly increased by the incorporation of $BaTiO_3$[Z. Liu, 2015], similarly the inclusion $Fe_3O_4$ content to PVDF/CNTs resulting in the enhancement of both electrical conductivity and dielectric permittivity of ternary nanocomposite prepared by twin screw compounding method [C. Tsonos, 2015]. The present work deals with a noval three-phase PVDF nanocomposite system with the loading of γ-SWCNTs and iron oxides Nanoparticles.

To be best of our knowledge there no systematic work on PVDF/γ-SWCNTs/$Fe_3O_4$ ternary nanocomposites in the literature. The effect of CNTs and $Fe_3O_4$ nanoparticles were especially studied in current research work. Focusing on the insulating behavior of PVDF and conductive role of the system by the incorporation of nanofillers.

**Materials and menthods**

*Chemicals and Material*

APVDF homopolymer in powder form ($M_w$=1, 82,000 g/mole), Sodium Hydroxide and ethanol were obtained from sigma-Aldrich and used without further purification. Dimethyle formamide (DMF) ($M_w$= 73.09 g/mole) and the additive single-walled carbon nanotubes were purchased from NANOCYL™ NC700 series having 90% purity and further modified through gamma radiation which was carried out at Pakistan Radiation service using $^{60}Co$ gamma irradiator (Model JS-7900, IR-148, and ATCOP) at dose rate of 1.02 kGy/h.were calculated through following equations [R. Gregorio,1994 A. Salimi, 2003].

$F_\beta = A_\beta / A_\beta + 1.26(A_\alpha)$..... (1)

$F_\alpha = A_\alpha / A_\alpha + 0.8(A_\beta)$..... (2)

Where $\mathbf{F_\beta}$ and $\mathbf{F_\alpha}$ are content fraction of amount of α and β- phase in PVDF nanocomposite sample, while $\mathbf{A_\beta}$and $\mathbf{A_\alpha}$ are correspond to their absorbance at 840 $cm^{-1}$ and 763 $cm^{-1}$.

*Preparation of Iron oxide Nanoparticles*

Magnetic nanoparticles were synthesized through co-precipitation method. Stirring of $FeCl_2.4H2O$ (2.0g), $Fe_3Cl_3.6H_2O$ (2.0g), in acidic media with deoxygenated $NH_4OH$ (250 $cm^3$, 1.5M).

The black precipitate was separated from solvent through magnetic decantation and washed with water and then two time with trimethyl ammonium hydroxide (100 $cm^3$. 0.1 M). The process was repeated three times. At the end the obtaining suspension was washed with organic solvent ethanol (Analytical grade) and kept it in a desiccator overnight for drying.

*Preparation of Nanocomposite*

Ternary nanocomposite system composed of PVDF with suitable additives (CNTs,$Fe_3O_4$) in desired loading range. The CNTs and $Fe_3O_4$ content were varying with respect to each other. Different kinds of binary and ternary nanocomposites were prepared through solution casting method. The details composition and formulation of the system is given in Table1. For composites synthesis, initially 1g of PVDF is added to 10 ml of DMF and stirred at room temperature and pressure at 600 rpm for two hours. After proper dissolution of PVDF in DMF, γ-SWCNTs (varying from 0.01g and 0.03g) were addedand the mixture is sonicated for six hours followed by five hours refluxed at 70°C at constant pressure.

The mixture were again sonicated for four hours at room temperature. Similar procedure wasfollowed for the rest of all mixtures where iron oxide nanoparticles (0.01 and 0.03g) and both additives with alternative concentration (0.01g of γ-SWCNTs and 0.03 $Fe_3O_4$, 0.03g of γ-SWCNTs and 0.01 $Fe_3O_4$)but sonication and refluxed time is increased by 1 hour. The mixture is than kept in oven for 1 hour at 100°C for the evaporation of solvent. The digital images of the prepared nanocomposites were shown in Fig.1.

*Characterization*

Morphology of the system was studied by Scanning Electron Microscopy (SEM) from the JEOL EM-10049 1200EX II electron microscope operating in high vacuum and their cross section was examined using an accelerating voltage of 10.0 kV.

FTIR analysis was carried out using FT-IR spectrophotometer (Nicolet 6700, Thermo Electron Crop, Waltham, Massachusetts, USA) at a scanning rate of 4000-500 $cm^{-1}$ (116 average scans) at resolution of 6.00 $cm^{-1}$ were taken during spectrum acquisition.

XRD analysis of the samples was performed at room temperature using X-rays diffractometer (Model STOE STADI P) with Cu-Kα radiation. The range of XRD from 2θ which are equal to 2 to 50°.

Thermal properties of the system were analyze by Mettler-Toledo TGA/SDTA851e (Scherzenbanh, Switzerland) with the heating rate of 20°C $min^{-1}$. Weight loss of the films were obtained from the curve. Electrical/dielectrical properties were studied by means of Impedance Spectroscopy. The dielectric permittivity were recorded and measured in a broad frequency ranged from 2 to 6 Hz.

**Results and discussion**

*Morphology*

Fig.2 (a-c) shows representative cross section SEM micrograph of the prepared nanocomposite system obtained at various magnifications. Fig.2 (a-c), is an indication of lake of agglomeration and presence of a good dispersion. The tubular structure in Fig.2 (a) represent the a good dispersion of CNTs while in Fig.2 (b) the small white dots which are presents and disperse throughout the matrix is sign of good dispersion of $Fe_3O_4$ nanoparticles.

**Table 1.** Formulation table with sample codes and the concentration of nanoparticles used.

| S.NO | Sample codes | PVDF (g) | γ-SWCNTs (g) | $Fe_3O_4$ (g) |
|---|---|---|---|---|
| 1. | AP-0 | 1 | 0 | 0 |
| 2. | APS-2 | 1 | 0.03 | 0 |
| 3. | APF-2 | 1 | 0 | 0.01 |
| 4. | AP-5 | 1 | 0.03 | 0.01 |

Similarly in Fig.2 (c) both types of additive are very well dispersed without significant agglomeration. Here diameter of $Fe_3O_4$ nanoparticles are in range of 60 nm.

*Fourier transform infrared spectroscopy (FT-IR)*

To study the chemical modification as well as to calculate the relative amount of β-phase PVDF FT-IR Spectroscopy was performed for PVDF powder, pure PVDF film and PVDF nanocomposites film as shown in Fig.3 (a-b). Fig. 3 (a) the bands are observed at 1403, 872, 761, 614, 486 $cm^{-1}$. The peaks at 761 and 486 $cm^{-1}$ are attributed to the α-phase while the peak at 872 are attributed to the γ-phase which confirms that there is no β-phase present in PVDF powder.The new peaks arise in PVDF film at 432, 513, 833, 1227 and 1734 $cm^{-1}$ attribute to the presence of β-phase and shifting of peak at 1399 $cm^{-1}$ to 1403 $cm^{-1}$ attribute to the presence of α-phase and 872 $cm^{-1}$ to the γ-phase.

**Table 2.** Percentage of α and β form PVDF.

| S.No | Codes | α % | β % |
|---|---|---|---|
| 1 | AP-0 | 50.80 | 49.19 |
| 2 | APS-2 | 49.74 | 50.25 |
| 3 | APF-2 | 50.85 | 49.14 |
| 4 | AP-5 | 50.53 | 49.46 |

This confirms the presence of α, β and γ-phases of crystalline phases in PVDF. Similar results was obtained by[T. Prabhakaran,2013]. Comparative analysis of pure PVDF film and PVDF composite were shown Fig. 3 (a) which shows the characteristic peaks for the existence of the three crystalline forms of PVDF. By the addition of $Fe_3O_4$ NPs some conformational changes were observed. It is cleared from the spectra, the peak at 1399 $cm^{-1}$ which is the characteristic of α-phase is getting weak, implying the reduction of α-phase crystallization in PVDF polymer, slightly shifting of peak 1399 $cm^{-1}$ to peak position 1403 $cm^{-1}$ as the amount of $Fe_3O_4$ NPs (0.01g) were added which confirms predominance of β- phase over α-phase. Addition of $Fe_3O_4$ NPs plays an important role of nuclie for PVDF crystallization which changes the kinetics of crystallization in such a way that contribution of β- phase increase and that of α-phase reduced. This confirms the predominance of β- phase over α-phase in composite, which enhanced the

polarization effects.

The shift in the 833 $cm^{-1}$ and 512 $cm^{-1}$ peaks seen from the spectra Fig.3 (b), insure the strong interaction of $Fe_3O_4$ NPs with PVDF matrix. It can be seen from the same spectra that $Fe_3O_4$ NPs led to considerable changes in the PVDF conformations but the change in γ-phase is not so significant but there are noticeable changes in α and β-phases. The relative amount of α and β-phase are given in Table 2.

**Table 3.** Peaks position for α, β, γ-phase of PVDF Nano composites with their respective functional groups.

| S.No | Codes | α-peaks $cm^{-1}$ | Assignment | β-peaks $cm^{-1}$ | Assignment | γ-peaks $cm^{-1}$ | Assignment |
|---|---|---|---|---|---|---|---|
| 1 | AP-0 | 615, 765, 1399 | $CF_2$ bending | 430, 834,512, 1272 | $CH_2$ rocking | 872, 1230 | $CH_2$ rocking, C-O stretching |
| 2 | APS-2 | 612,763, 1403 | $CF_2$ bending | 427, 510, 833, 1274 | $CH_2$ rocking | 872, 1230 | $CH_2$ rocking, C-O stretching |
| 3 | APF-2 | 612, 763, 1399 | $CF_2$ bending | 431, 512, 833, 1273 | $CH_2$ rocking | 872, 1230 | $CH_2$ rocking, C-O stretching |
| 4 | AP-5 | 612, 763, 1401 | $CF_2$ bending | 430, 512, 835, 1272 | $CH_2$ rocking | 872, 1230 | $CH_2$ rocking, C-O stretching |

It is also observed from Fig. 3(b) that the decreased in the absorption band of α-phase at peak 1399 $cm^{-1}$ gets weaken with the addition of γ-SWCNT (0.03g) coded as APS-2, which indicates that the formation β-phase is significantly dependent upon concentration of γ-SWCNT because γ-SWCNT is a strong nucleophile and the fluorine is strong electrophile so it has the capability to attract the electron. The spectra also show the shifting on peak at 512 $cm^{-1}$ and 1227 $cm^{-1}$ which shows strong interaction γ-SWCNT with PVDF. Two distinct absorption peaks for β-phase are observed at 508 $cm^{-1}$ and 827 $cm^{-1}$. The peaks positions for α, β γ-phase of PVDF nanocomposites are listed in Table 3.

**Table 4.** Percentage of weight remaining at different temperature.

| Percentage of weight remaining | | | | |
|---|---|---|---|---|
| Serial No | Sample codes | 450-460°C | 475-500°C | 810°C |
| 1 | AP-5 | 90.9 % | 40.4 % | 29.6 % |
| 2 | APF-2 | 90.9 % | 33 % | 14.1 % |
| 3 | APS-2 | 91.2 % | 46 % | 22.4 % |

Addition of $Fe_3O_4$ NPs in PVDF/CNTs which is coded as AP-5 in Figure 3.2 (b), have also effective in changing the phase conformation from α and β-phases. But from these result it is clear that it is mainly the CNTs which have strong capability of promotion of β- phase from α-phase [P.Martins,2012,P.Martins,2011].

*X-ray diffraction (XRD)*

X-ray diffraction (XRD) have often used to determine the phases of PVDF as well as the interaction of filler with the matrix. Fig.4. (a) shows the crystalline peak at 2θ = 18.4° and 2θ = 20° which correspond to the crystalline plane (020) and (110) and there is no peak found for β-phase PVDF which confirm that the PVDF exist in α-phase. In Fig. 4 (b) APS-2 confirms the presence of β-phase which refer to crystalline plane (110)/(200) of β-phase. The peak which specially represent the existence of α-phase at 2θ = 17.8°, 18.4°, 26.8° for α-phase PVDF are completely absent in all type of nanocomposites.

Fig. 5(C) shows nanocomposite of PVDF with $Fe_3O_4$ NPs (0.01g) and ternary nanocomposite γ-SWCNTs/$Fe_3O_4$ (0.03/0.01g) are coded as APF-2 and AP-5 respectively.

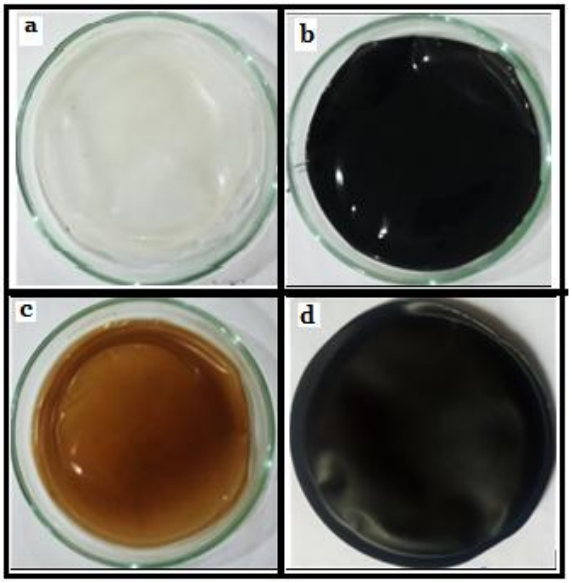


**Fig. 1.** Different types of films (a) AP-0 as blank (b) APS-2 (c) APF-2 (d) AP-5.

The addition of $Fe_3O_4$ led to the phase change of PVDF from α-phase to β-phase. It also shows the crystalline peak at 2θ = 20.3° and 2θ = 42.8° attribute to the crystalline plane (110/020) and (400) which are the characteristic peaks for β-phase PVDF, It can be noted that loading with $Fe_3O_4$ NPs increase the total crystallinity of PVDF matrix.

The peak at 2θ = 35.7° is due to the incorporation of $Fe_3O_4$ NPs corresponding to the crystalline plane (311) which are the characteristic of $Fe_3O_4$ nanoparticles as well as an indication for the cubic spinal structure of $Fe_3O_4$ NPs. It also shows the interaction of $Fe_3O_4$ NPs with PVDF matrix. There is no new peak found in the XRD pattern of PVDF/$Fe_3O_4$ except for those of PVDF and $Fe_3O_4$ NPs which shows that there is no new phase produced. Same result are produced by Prabakar *et al.* [T. Prabhakaran, 2013].

Figure.3.4 (d) have the alternating concentration of the fillers γ-SWCNTs (0.03g) and $Fe_3O_4$ (0.01g) which shows the significant shift of the peak from 2θ = 20.3° which are present in both APS-2 and APF-2 to 2θ = 20.5° refer to the crystalline plane (110)/(200) which is an indication of the more prominent β-phase of PVDF. The peak arise at 2θ = 36.5° refer to the crystalline plane (311) is an indication of interaction of $Fe_3O_4$ NPs with PVDF matrix.

The new peak at 2θ = 43.1 shows the mutual interaction of γ-SWCNTs with $Fe_3O_4$ NPs correspond to crystalline plane (101).

*Thermal analysis*

Thermal stability is increase when nanofiller is added to PVDF matrix which are shown in Fig.6.It is clear from Figure that there is a two steps degradation process.

The first step shows the evaporation of absorbed moisture and the solvent. The second step is an indication for the major weight loss occurred in the range 450 to 510°C which refer to the degradation of main polymer chain. PVDF composite for AP-5 the degradation temperature for the major weight loss is 490°C which might be due the oxidation of the γ-SWCNTs and as well as due to proper dispersion the $Fe_3O_4$ filler.

The weight loss in APF-2 at temperature 498°C shows the strong electrostatic interaction of filler with the matrix while in APS-2 the major weight loss is occurred at 479°C which show theoxidation of γ-SWCNT with the PVDF matrix. Loading of PVDF with the filler shows an increase in thermal stability of the nanocomposite. Prabakar *et al* reported 452°C as the degradation temperature of pure PVDF film. The enhancement in thermal degradation of PVDF nanocomposites is also an evidence for the interaction of nanofiller with the matrix.

Residual weight percent remaining at different temperature for all nanocomposite are shown in Table 4.

*Dielectric and electrical properties*

Dielectric permittivity of the PVDF samples are shown in Fig.7. Dielectric permittivity of the neat PVDF film AP-0 at lower frequency (2 Hz) is -0.9 which is increasing constantly with the increase in frequency up to its maximum -0.06 at the frequency range of 6 Hz.

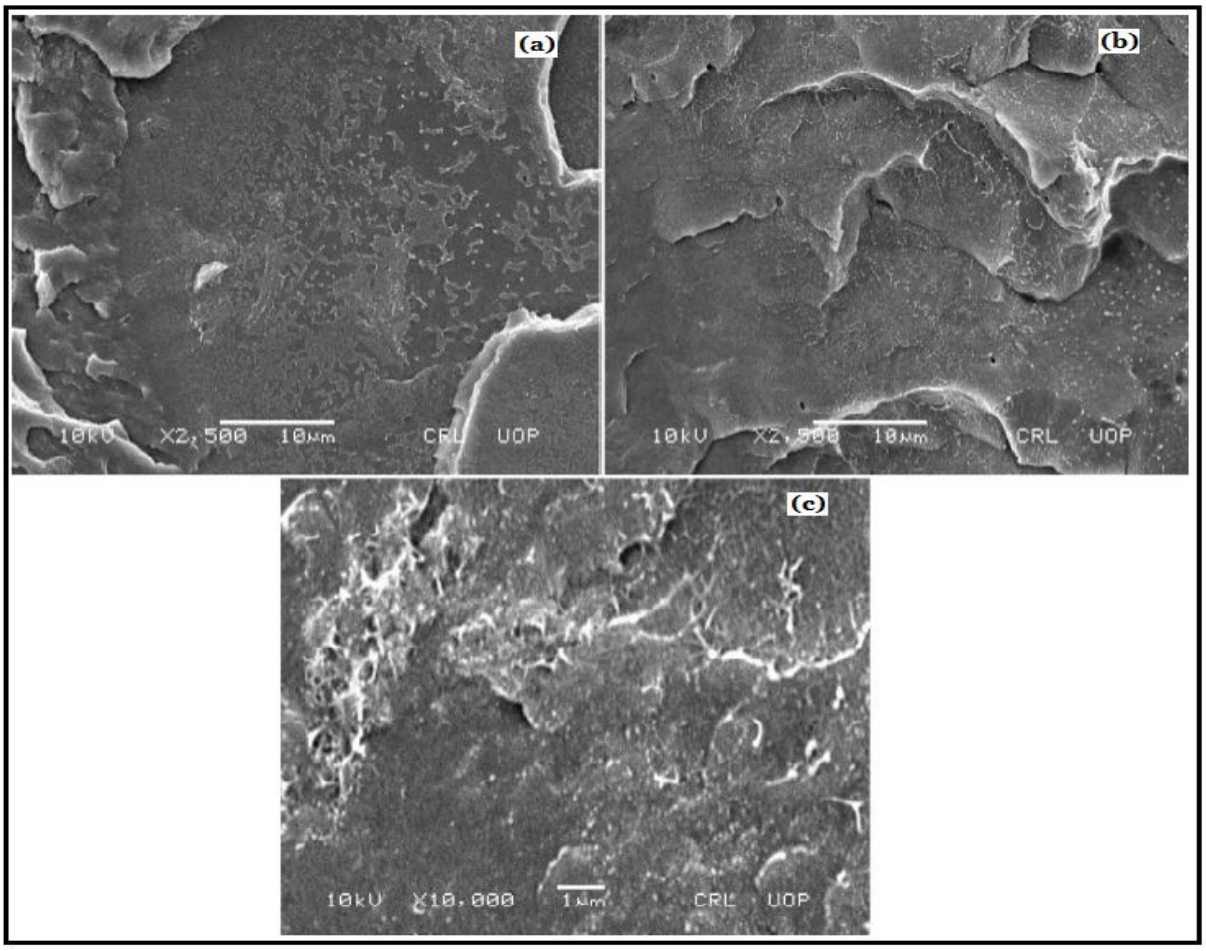


**Fig. 2.** Scanning electron microscopy of nanocomposite film (a) APS-2 (b) APF-2 (C) AP-5.

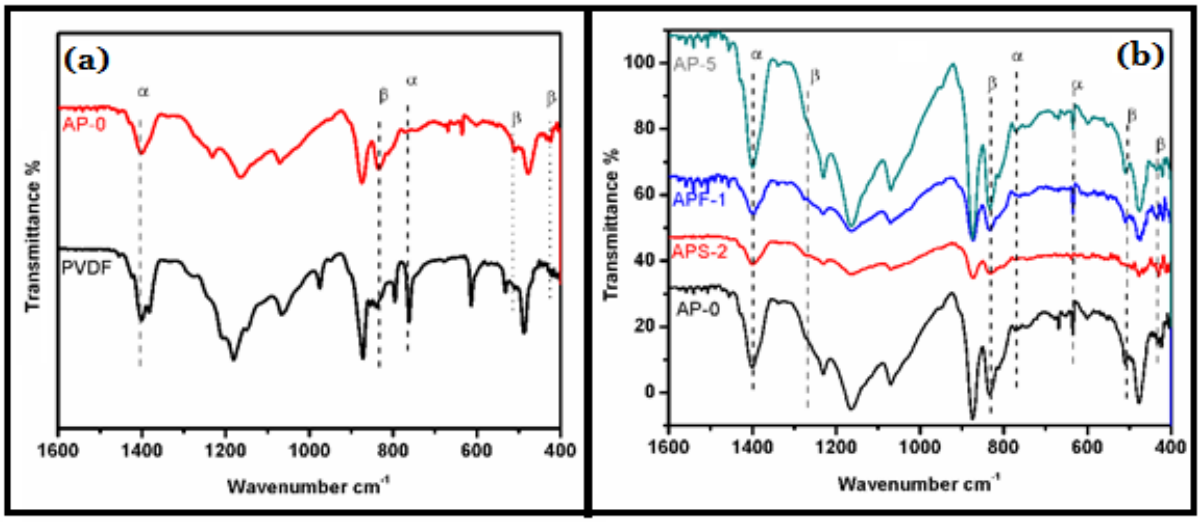


**Fig. 3.** FT-IR spectra of (a) PVDF powder and neat film (b) neat film and PVDF nanocomposites film.

When the nanofiller is mixed with the PVDF matrix the dielectric permittivity of the nanocomposites are increased significantly. A huge increase in dielectric permittivity of PVDF/ γ-SWCNTs nanocomposite APS-2 is observed at lower frequency range 2 Hz to be 6.1 largely due to the interaction of CNTs with the PVDF matrix. It is interesting to note that the dielectric permittivity of the nanocomposite is higher than PVDF matrix is evidence for the strong interaction of CNTs with PVDF matrix. So according to Maxwell-Wagner-Seller effect "the charge can be accumulated at the interface of two dielectric

materials with different relaxation time when the current flow across the material interfaces. The relaxation time of the PVDF is several orders of magnitude larger than CNTs. Therefore, the charge carrier is blocked at the interfaces due to MWS effect, so enhancing the dielectric permittivity significantly. Meanwhile the donor-acceptor complexes are also formed at the interface of PVDF and γ-SWCNTs, so the MWS effect can be intensified greatly, that is the delocalized π-electron cloud of CNTs and the electrophile "F" group strongly attract these electrons [Z. Liu,2015].

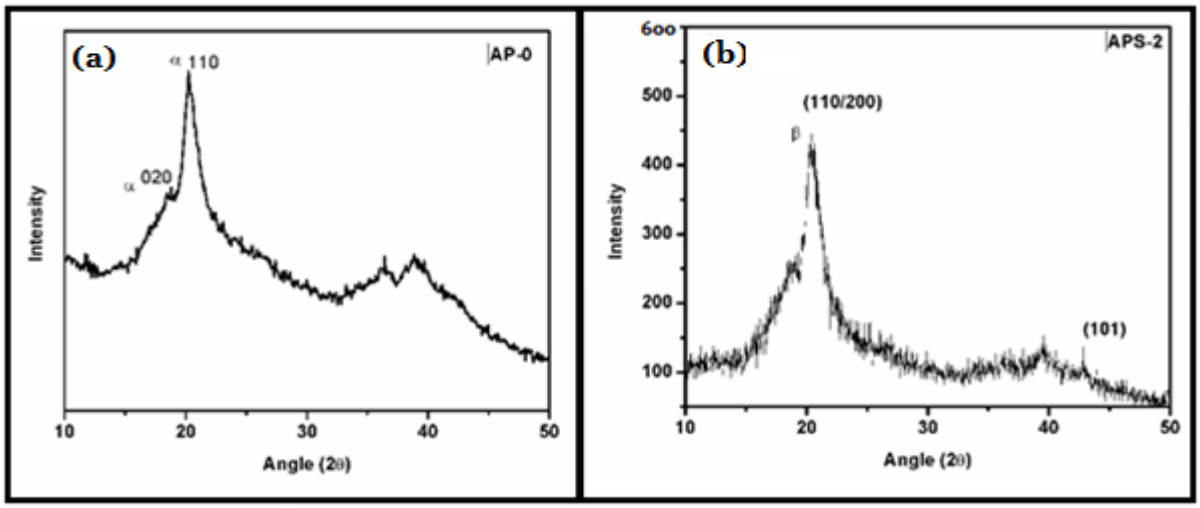


**Fig. 4.** (a) PVDF neat film (b) PVDF/ γ-SWCNTs nanocomposite.

Furthermore, a thin insulting layer of semi-crystalline PVDF is combined with the CNTs to form nanocomposite. This structure fully shows the advantage of γ-SWCNTs and resulting a huge interfacial area between γ-SWCNTs and PVDF in the nanocomposite, which in turn provides numerous sites for reinforced MWS effect [J.-K. Yuan, 2011].

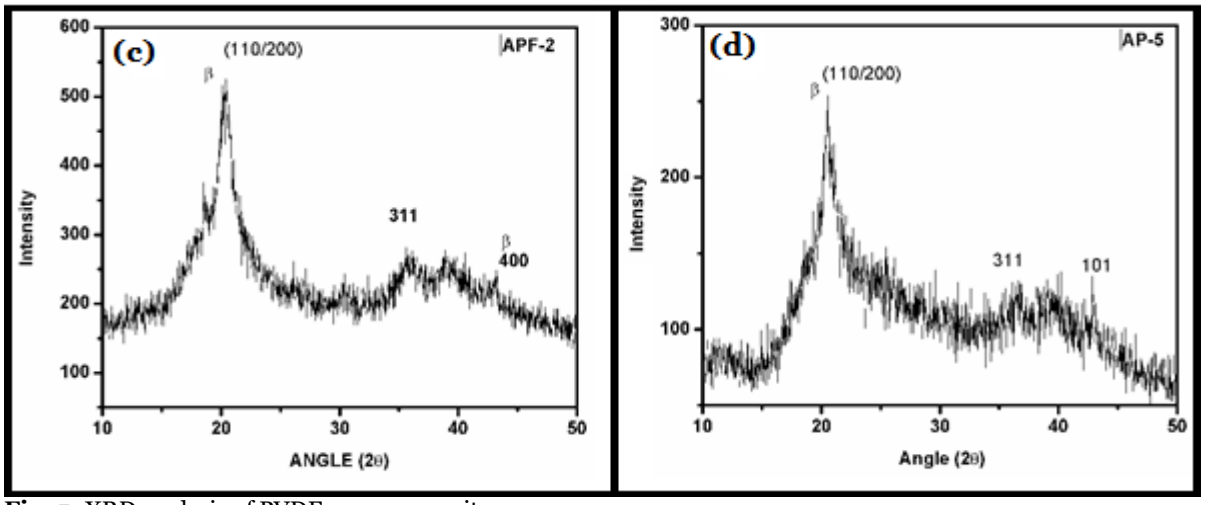


**Fig. 5.** XRD analysis of PVDF nanocomposites.

Now as the $Fe_3O_4$ nanoparticles are added to PVDF matrix it has also an effect on the permittivity of the nanocomposites of the PVDF matrix, the huge increase of dielectric permittivity is occurred due to proper dispersion and strong interaction of the nanoparticles with the matrix. As the $Fe_3O_4$ nanoparticles are added the value of dielectric permittivity increased significantly to 5.8 at the lower frequency range 2 Hz.

It is obvious that the $Fe_3O_4$ nanoparticles play an important role on the dielectric properties of composite with the increase in ε' value (for 0.03g of $Fe_3O_4$) caused by increasing the interfacial space-charge polarization between the polymer matrix PVDF and nanoparticles.

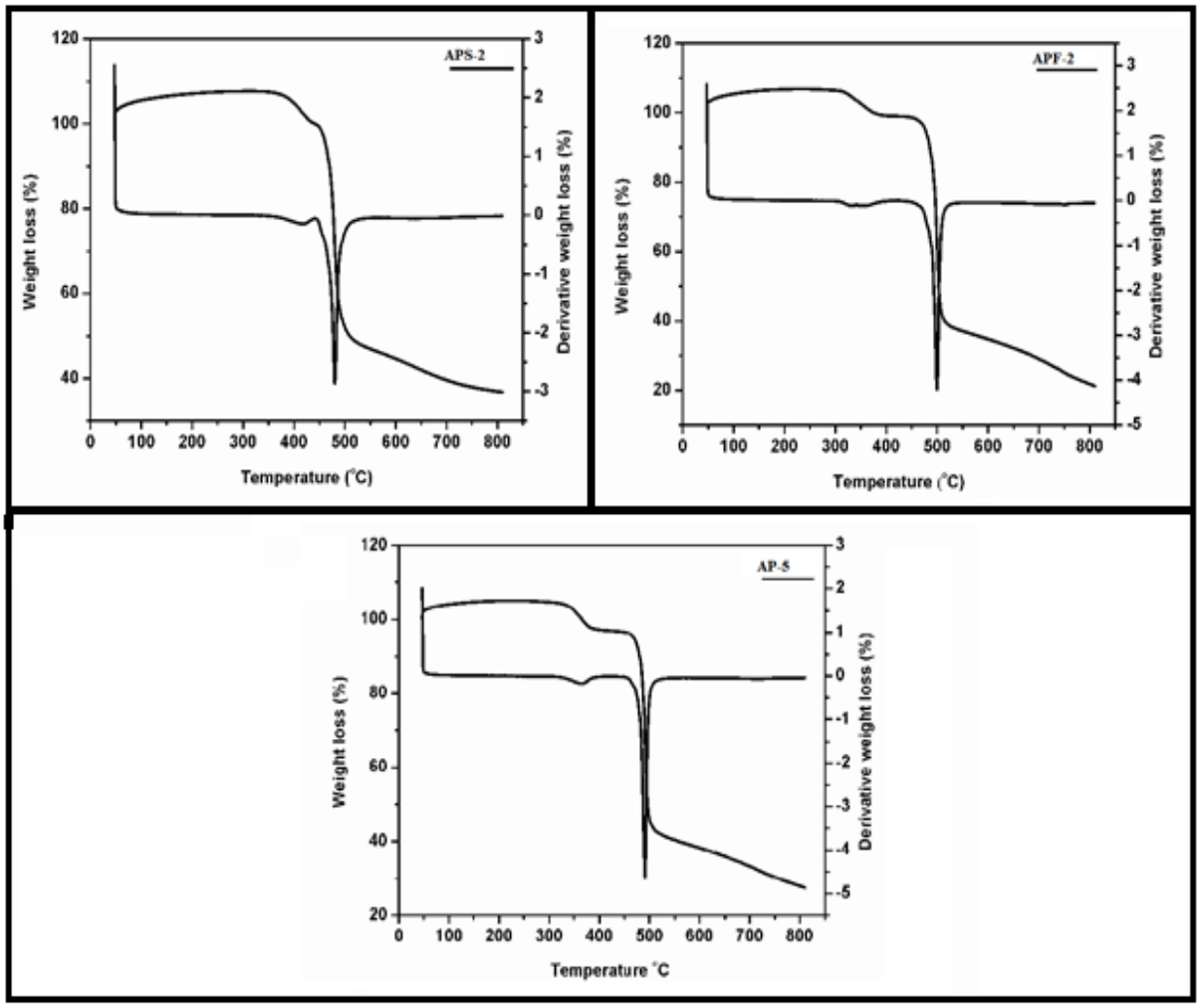


**Fig. 6.** Thermal analysis of nanocomposites TGA and DTA curve.

For ternary nanocomposite which are coded as AP-5 in Fig. 7 where 0.01g $Fe_3O_4$ nanoparticles are added to PVDF/ γ-SWCNTs matrix. It is clear from the graph that there is no effect of the less concentration of $Fe_3O_4$ on the dielectric permittivity of PVDF/ γ-SWCNTs/ $Fe_3O_4$ as compared to PVDF/ γ-SWCNTs nanocomposite. Here the huge increase in the dielectric permittivity to 6.1 at the frequency range 2 Hz shows the dominance of γ-SWCNTs over $Fe_3O_4$ nanoparticles in the nanocomposite. The high value of dielectric permittivity at CNTs content attribute due the presence of large number of nanocapacitor structure with large interfacial polarization with high dipole moment, where γ-SWCNTs acts as the nanoelectrodes and PVDF as nanodielectrics, experiencing interfacial polarization [M. Arjmand, 2012 L. Wang, 2005].

Fig.8 shows the dielectric constant (k) value for neat PVDF film dielectric value are found to be -0.8 at 2 Hz which are increased linearly with the increase in frequency and reached to its maximum value -0.04 at 6 Hz the lower value for dielectric constant indicates that there is no interface formation and the absence of space for storage of charge in insulating material.

On reinforcing PVDF with 0.03g of γ-SWCNTs, dielectric value is increased significantly to 6.1at lower frequency 2 Hz and shows almost linear behavior as the frequency increased. This huge increased in dielectric constant value for the

nanocomposite of PVDF is due to the fact that there is a strong interaction between γ-SWCNTs and PVDF matrix, interface is created and the mobile charge carrier are accumulated.

As $Fe_3O_4$ nanoparticles are mixed in PVDF matrix the value of dielectric constant is again very high that is 5.6 at 2 Hz as compared to PVDF matrix and remain almost constant as the frequency increased. It might be due to MWS effect which are discussed already. The lower value of dielectric constant of PVDF/$Fe_3O_4$ as compared to PVDF/ γ-SWCNTs might be due to the tendency of $Fe_3O_4$ nanoparticles toward agglomeration. So, the insulating gap in PVDF are high in PVDF/$Fe_3O_4$ as compared to PVDF/ γ-SWCNTs nanocomposite.

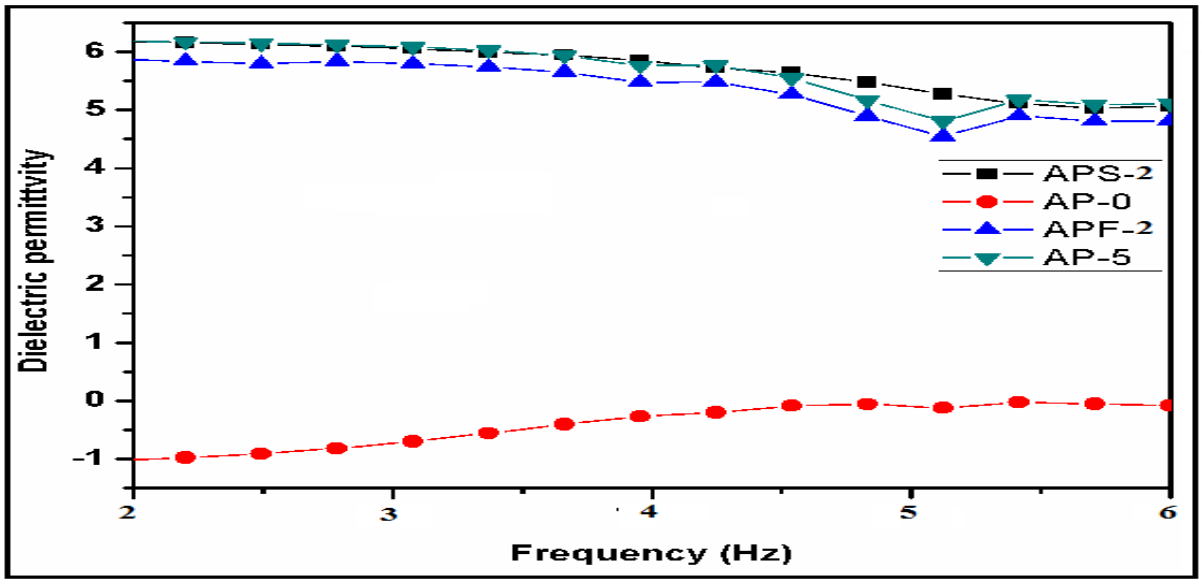


**Fig. 7.** Dielectric permittivity of PVDF nanocomposite film.

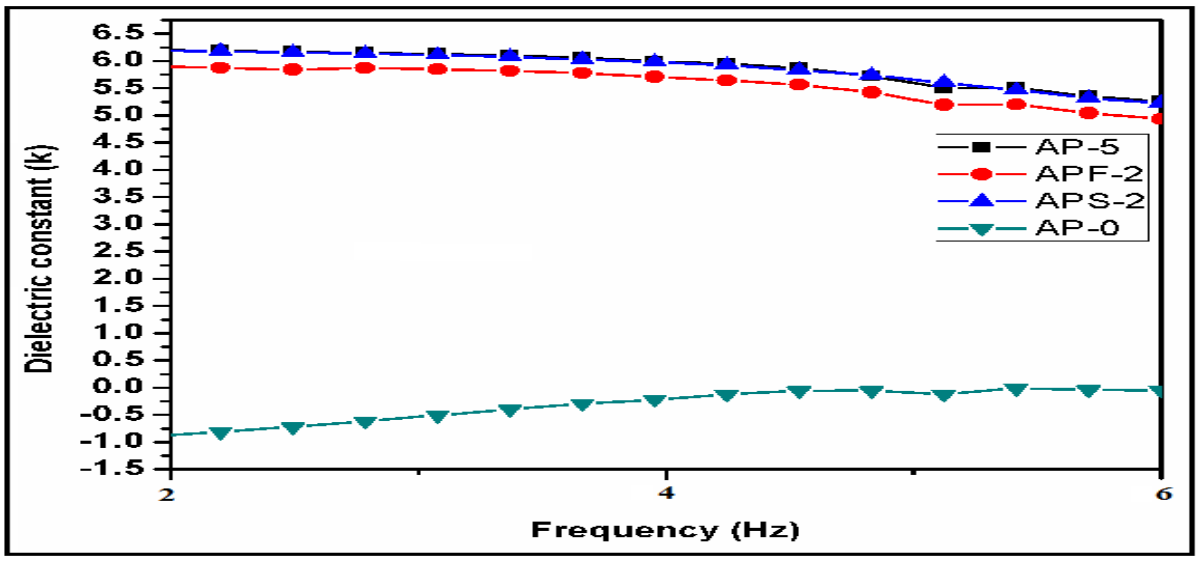


**Fig. 8.** Dielectric constant of PVDF nanocomposites film.

For ternary nanocomposite the dielectric value is raised up to 6.1 at the lower frequency which is almost equal to PVDF/ γ-SWCNTs nanocomposite and shows a linear behavior but a sudden drop in dielectric value from 6.1 to 5.3 at a frequency 5.5 Hz shows the presence of $Fe_3O_4$ nanoparticles. It is also observed that the dielectric value is again increased which shows the dominancy of γ-SWCNTs over $Fe_3O_4$ nanoparticles in ternary nanocomposite.

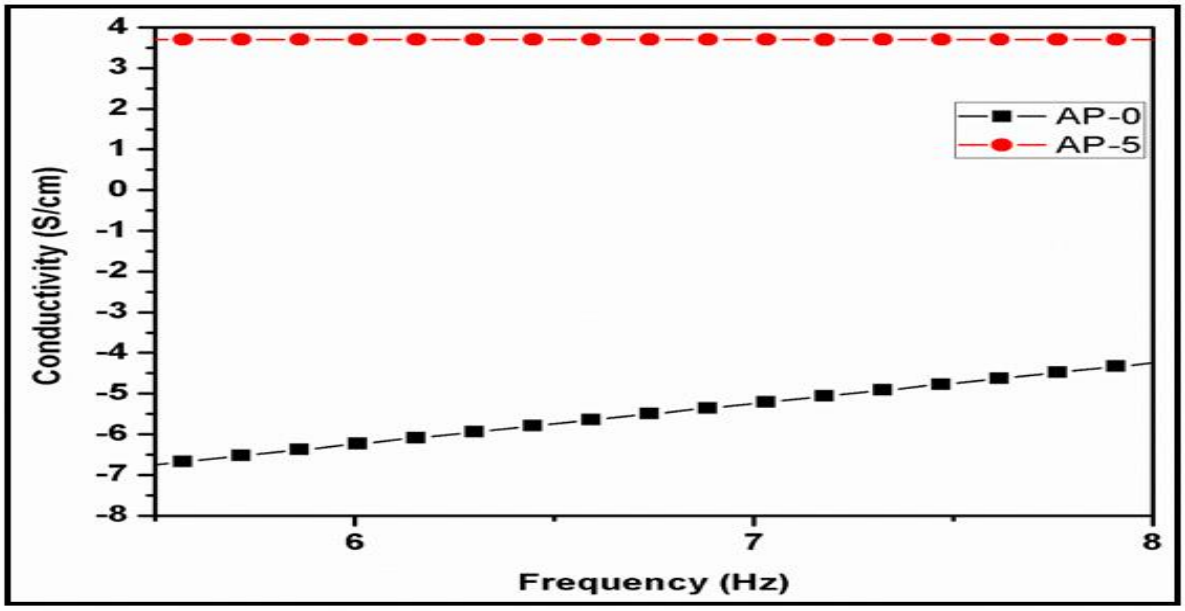


**Fig. 9.** Conductivity of PVDF nanocomposites films.

Fig.9 shows the conductivity spectra of PVDF with loading of γ-SWCNTs and $Fe_3O_4$ nanoparticles as a function of frequency. The conductivity of PVDF increase by loading with nanofiller from -6.8 S/cm for pristine to 3.7 S/cm for ternary nanocomposite at 5.5 Hz. It shows a linear behavior independent of frequency.

## Conclusion

In this study different type of PVDF nanocomposite films were synthesized by solution casting method using different weight percent of nanofillers. The nanocomposite samples were characterized by different techniques including Scanning electron microscopy (SEM) which confirm the proper interaction and distribution of the nanofiller with PVDF matrix. Ternary nanocomposite also shows good distribution and provide a good nucleation surrounding for PVDF, (FT-IR) shows the conversion of α-phase to β-phase. Decrease in percent transmittance confirms the interaction of nanofiller with matrix. X-rays diffraction shows that pure PVDF is present in α-phase because the popular peaks present are 2θ=18.4°, 2θ=20°, by adding nanofiller the peaks are shift to 2θ=20.3°, for ternary nanocomposite the most prominent β-phase is achieved i.e. 2θ=20.5°. It is well known that degradation temperature of pure PVDF film is 452°C. It is proved from thermo gravimetric analysis that the Nano composite of PVDF become thermally stable.

It can be noted, the huge increase in value of dielectric permittivity due the presence of both $Fe_3O_4$ and CNTs by creating the interfacial space which have capability for storing the charges, a behavior interesting for electronic devices. Similarly, the dielectric constant value is also increased due the donor-acceptor complex formation between the Nano filler and the matrix. For ternary nanocomposite the conductivity is also increased shows the dominancy of CNTs because no restriction to charge barrier due to $Fe_3O_4$ NPs and shows a linear behavior independent of frequency. Ternary nanocomposite is a very promising system in the field of conducting devices.

## Acknowledgment

Oneof the author is acknowledge to Dr. Saira bibi, Mam saddiqa Bigam and Dr. Mohsan Nawaz for their fruitful co-operation and suggestions. I am also very thankful to Department of Chemistry, Hazara University Mansehra for providing the research facilities.

## Reference

**Lovinger AJ.** 1983. Ferroelectric polymers, Science **220,** p 1115-1121.

**Salimi A, Yousefi A.** 2003. Analysis method: FTIR studies of β-phase crystal formation in stretched PVDF films, Polymer Testing **22,** p 699-704.

**Bhatt AS, Bhat DK, Santosh M.** 2011. Crystallinity, conductivity, and magnetic properties of PVDF-$Fe_3O_4$ composite films, Journal of Applied Polymer Science **119,** p 968-972.

**Tsonos C, Pandis C, Soin N, Sakellari D, Myrovali E, Kripotou S.** 2015. Multifunctional nanocomposites of poly (vinylidene fluoride) reinforced by carbon nanotubes and magnetite nanoparticles, Express Polymer Letters **9.**

**Prinz GA.** 1998. Magnetoelectronics, Science,vol. **282,** p 1660-1663.

**Kim GH, Hong SM, Seo Y.** 2009. Piezoelectric properties of poly (vinylidene fluoride) and carbon nanotube blends: β-phase development, Physical chemistry chemical physics **11,** p 10506-10512.

**Kawai H.** 1969. The piezoelectricity of poly (vinylidene fluoride), Japanese Journal of Applied Physics **8,** p 975.

**Bergman Jr J, McFee J, Crane G.** 1971. Pyroelectricity and optical second harmonic generation in polyvinylidene fluoride films, Applied Physics Letters **18,** p 203-205.

**Kumar J, Singh RK, Samanta SB, Rastogi RC, Singh R.** 2006. Single-Step Magnetic Patterning of Iron Nanoparticles in a Semiconducting Polymer Matrix, Macromolecular chemistry and physics **207,** p 1584-1588.

**Yuan JK, Yao SH, Dang ZM, Sylvestre A, Genestoux M, Bai1 J.** 2011. Giant dielectric permittivity nanocomposites: realizing true potential of pristine carbon nanotubes in polyvinylidene fluoride matrix through an enhanced interfacial interaction, The Journal of Physical Chemistry C **115,** p 5515-5521.

**Wang L, Dang ZM.** 2005. Carbon nanotube composites with high dielectric constant at low percolation threshold, Applied physics letters **87,** p 042903.

**Wang M, Shi JH, Pramoda K, Goh SH.** 2007. Microstructure, crystallization and dynamic mechanical behaviour of poly (vinylidene fluoride) composites containing poly (methyl methacrylate)-grafted multiwalled carbon nanotubes," Nanotechnology **18,** p 235701.

**Arjmand M, Apperley T, Okoniewski M, Sundararaj U.** 2012. Comparative study of electromagnetic interference shielding properties of injection molded versus compression molded multi-walled carbon nanotube/polystyrene composites, Carbon **50,** p 5126-5134.

**Levi N, Czerw R, Xing S, Iyer P, Carroll DL,** 2004. Properties of polyvinylidene difluoride– carbon nanotube blends, Nano Letters **4,** p 1267-1271.

**Bajpai O, Setua D, Chattopadhyay S.** 2015. A Brief Overview on Ferrite (Fe3O4) Based Polymeric Nanocomposites: Recent Developments and Challenges, Journal of Research Updates in Polymer Science **3,** p 184-204.

**Martins P, Lopes A, Lanceros-Mendez S.** 2014. Electroactive phases of poly (vinylidene fluoride): determination, processing and applications, Progress in polymer science **39,** p 683-706.

**Martins P, Costa CM, Botelho G, Lanceros-Mendez S, Barandiaran J, Gutierrez J.** 2012. Dielectric and magnetic properties of ferrite/poly (vinylidene fluoride) nanocomposites, Materials Chemistry and Physics **131,** p 698-705.

**Martins P, Costa CM, Lanceros-Mendez S.** 2011. Nucleation of electroactive β-phase poly (vinilidene fluoride) with $CoFe_2O_4$ and $NiFe_2O_4$ nanofillers: a new method for the preparation of multiferroic nanocomposites, Applied Physics A,

**103,** p233-237.

**Gregorio Jr R, Cestari M.** 1994. Effect of crystallization temperature on the crystalline phase content and morphology of poly (vinylidene fluoride), Journal of Polymer Science Part B: Polymer Physics **32,** p 859-870.

**Begum S, Kausar A, Ullah H, Siddiq M.** 2016. Potential of Polyvinylidene Fluoride/Carbon Nanotube Composite in Energy, Electronics, and Membrane Technology: An Overview, Polymer-Plastics Technology and Engineering **55,** p 1949-1970.

**Zhang S, Zhang N, Huang C, Ren K, Zhang Q.** 2005. Microstructure and electromechanical properties of carbon nanotube/poly (vinylidene fluoride—trifluoroethylene—chlorofluoroethylene) composites, Advanced Materials **17,** p 1897-1901.

**Manna S, Mandal A, Nandi AK.** 2010. Fabrication of Nanostructured Poly (3-thiophene methyl acetate) within Poly (vinylidene fluoride) Matrix: New Physical and Conducting Properties, The Journal of Physical Chemistry B **114,** p 2342-2352.

**Prabhakaran T, Hemalatha J.** 2013. Ferroelectric and magnetic studies on unpoled Poly (vinylidine Fluoride)/$Fe_3O_4$ magnetoelectric nanocomposite structures, Materials Chemistry and Physics **137,** p 781-787.

**Furukawa T.** 1989. Ferroelectric properties of vinylidene fluoride copolymers,"Phase Transitions: A Multinational Journal **18,** p 143-211.

**Sencadas V, Moreira MV, Lanceros-Méndez S, Pouzada AS, Gregório Filho R.** 2006. α-to β Transformation on PVDF films obtained by uniaxial stretch, in Materials science forum p 872-876.

**Eerenstein W, Mathur N, Scott JF.** 2006. Multiferroic and magnetoelectric materials, nature **442,** p 759.

**Zhang WB, Zhang Zx, Yang JH, Huang T, Zhang N, Zheng XT.** 2015. Largely enhanced thermal conductivity of poly (vinylidene fluoride)/carbon nanotube composites achieved by adding graphene oxide, Carbon **90,** p 242-254.

**Gu X, Michaels C, Nguyen D, Jean Y, Martin J, Nguyen T.** 2006. Surface and interfacial properties of PVDF/acrylic copolymer blends before and after UV exposure, Applied surface science **252,** p 5168-5181.

**Wang X, Li W, Luo L, Fang Z, Zhang J, Zhu Y,** 2012. High dielectric constant and superparamagnetic polymer-based nanocomposites induced by percolation effect, Journal of Applied Polymer Science **125,** p 2711-2715.

**Fu Y, Harvey EC, Ghantasala MK, Spinks G. M.** 2005. Design, fabrication and testing of piezoelectric polymer PVDF microactuators, Smart materials and structures **15,** p S141.

**Liu Z, Feng Y, Li W.** 2015. High dielectric constant and low loss of polymeric dielectric composites filled by carbon nanotubes adhering $BaTiO_3$ hybrid particles, RSC Advances **5,** p 29017-29021.